A&A 378, L45–L48 (2001)
DOI: 10.1051/0004-6361:20011265

Astronomy & Astrophysics

Letter to the Editor

Deep spectroscopy of the low-metallicity blue compact dwarf galaxy SBS 0335–052*

Y. I. Izotov[1], F. H. Chaffee[2], and D. Schaerer[3]

[1] Main Astronomical Observatory, Ukrainian National Academy of Sciences, Golosiiv, Kyiv 03680, Ukraine
[2] W. M. Keck Observatory, 65-1120 Mamalahoa Hwy., Kamuela, HI 96743, USA
[3] Observatoire Midi-Pyrénées, Laboratoire d'Astrophysique, UMR 5572, 14 Av. E. Belin, 31400 Toulouse, France

Received 1 August 2001 / Accepted 10 September 2001

Abstract. The results of deep long-slit spectroscopy of the extremely low-metallicity blue compact dwarf (BCD) galaxy SBS 0335–052 are presented. Down to intensity levels of $10^{-3\cdots-4}$ of Hβ, unprecedented for spectroscopy of extra-galactic giant H II regions, we detect numerous weak permitted and forbidden nebular lines in the brightest part of the galaxy. With varying degrees of confidence, the detections include lines of high-ionization ions like Fe^{4+}–Fe^{6+}, implying very hard ionizing radiation. Two broad emission features, possibly from Wolf-Rayet stars, and stellar He II λ4200 absorption are seen in the same region. The large spatial extent of He II λ4686 emission (implying the presence of sufficient ionizing photons with energies above 54 eV) and the spatial distribution of the electron temperature suggest that at least some part of the hard radiation is associated with shocks. Extended Hα emission is detected over ∼6–8 kpc, a much larger area than in previous studies, suggesting that hot ionized gas is spread out far away from the central ionizing clusters. This shows that nebular line and continuous emission can significantly modify the colours of these extended regions and must be taken into account in studies of the underlying stellar population.

Key words. galaxies: fundamental parameters – galaxies: starburst – galaxies: individual (SBS 0335–052)

1. Introduction

Since its discovery by Izotov et al. (1990) as a very metal-poor galaxy the blue compact dwarf (BCD) galaxy SBS 0335–052 (SBS – the Second Byurakan Survey) has been studied extensively. The oxygen abundance in SBS 0335–052 is 12 + log O/H = 7.30 (Melnick et al. 1992; Izotov et al. 1997, 1999) and places it after I Zw 18 as the second most metal-deficient BCD. The properties of SBS 0335–052 as a probable young galaxy are of great interest for cosmology (e.g., Izotov et al. 1997). Therefore, detailed studies of this galaxy can shed light on the formation and the properties of the high-redshift primeval galaxies. Using deep spectroscopic observations we concentrate in the present paper on two problems: (1) the origin of very hard radiation at wavelengths shorter 228 Å. This radiation is indicated by the presence of the strong He II λ4686 emission line (Izotov et al. 1997) and implies that some other weak emission lines of high-ionization species could be present in the spectrum of SBS 0335–052. (2) the analysis of the properties of extended emission around SBS 0335–052. This problem is of great importance in understanding the evolutionary status of SBS 0335–052. In particular, we aim to understand how important gaseous emission is in SBS 0335–052 and how far it extends from the ionizing clusters.

2. Observations and data reduction

The observations of SBS 0335–052 were carried out on January 9, 2000 on the Keck II telescope with the low-resolution imaging spectrograph (LRIS) (Oke et al. 1995), using the 300 groove mm^{-1} grating which provides a dispersion 2.52 Å $pixel^{-1}$ and a spectral resolution of about 8 Å in first order. The slit was $1'' \times 180''$, centered on the brightest H II region and oriented along the major axis with a position angle PA = −30°. No binning along the spatial axis has been done, yielding a spatial sampling of $0\farcs2$ $pixel^{-1}$. The total exposure time was 60 min, broken into four 15 min exposures. All exposures were taken at an airmass of 1.1. The seeing was $0\farcs9$. Wavelength calibration was provided by Hg-Ne-Ar comparison lamp spectra obtained after each exposure. Two spectrophotometric standard stars, Feige 34 and HZ 44, were observed for flux calibration. The data reduction was made with the IRAF[1]

Send offprint requests to: Y. I. Izotov,
e-mail: `izotov@mao.kiev.ua`

* Data contained herein were obtained at the W. M. Keck Observatory which is operated as a scientific partnership among the California Institute of Technology, the University of California and the National Aeronautics and Space Administration. The Observatory was made possible by the generous financial support of the W. M. Keck Foundation.

[1] IRAF is the Image Reduction and Analysis Facility distributed by the National Optical Astronomy Observatory, which is operated by the Association of Universities for Research in Astronomy (AURA) under cooperative agreement with the National Science Foundation (NSF).

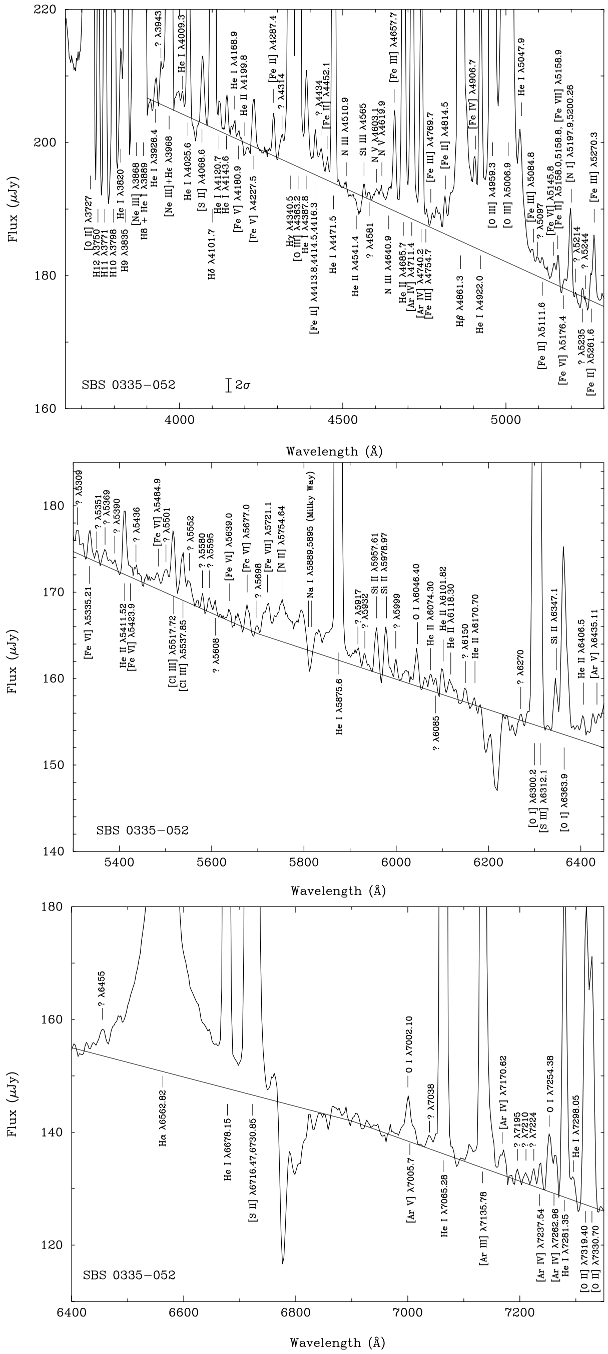

Fig. 1. The spectrum of the brightest region with line identifications. On each panel a continuum is drawn by hand to guide the eye. 2σ error in the continuum placement is shown in the upper panel.

software package. The two–dimensional spectra were bias–subtracted and flat–field corrected. Cosmic-ray removal, wavelength calibration, night sky background subtraction, correction for atmospheric extinction and absolute flux calibration were then performed.

For the analysis of spatial distribution of the brightest emission lines we also use the Keck spectrum of SBS 0335–052 obtained earlier by Izotov et al. (1999) at a position angle of 80°.

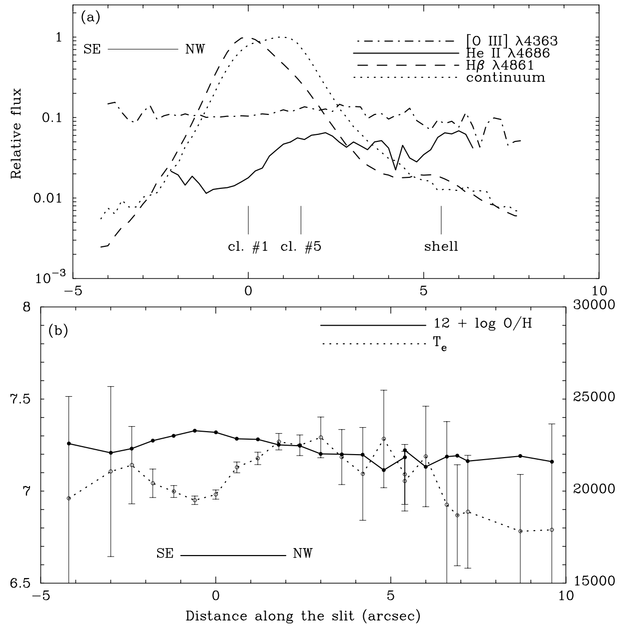

Fig. 2. a) The spatial distributions along the slit of the relative fluxes of the emission lines and continuum near Hβ. The fluxes of the Hβ emission line and continuum are normalized to their maximum values, while the fluxes of [O III] λ4363 and He II λ4686 are relative to the flux of Hβ. The slit is oriented at position angle PA = $-30°$. Origin is set at the maximum flux of the Hβ emission line. **b)** The spatial distribution of the electron temperature $T_{\rm e}$ and oxygen abundance 12 + log O/H.

A distance of 54 Mpc to SBS 0335–052 is adopted throughout this paper (Izotov et al. 1997). At this distance, 1″ corresponds to 260 pc.

The spectrum of the brightest region in a 1″×2.″2 aperture with secure and tentative line identifications (see below) is shown in Fig. 1. The measured S/N is of the order of 100. Extinction-corrected fluxes of the emission lines normalized to the flux of $10^{-4}\times I$(Hβ) are shown in Table 1.

3. Weak nebular emission and stellar absorption lines

One of main results (see Fig. 1) is the detection of numerous weak permitted and forbidden emission lines, which are – to the best of our knowledge – detected for the first time in the spectrum of an extra-galactic giant H II region. Lines with fluxes down to ∼0.1% of Hβ are clearly detected. For weaker lines the identifications are tentative and the measured fluxes are fairly uncertain, with relative errors ∼100%, while the relative errors of the fluxes for the strongest lines are ∼1%. Thirty unidentified emission features with fluxes 0.02%–0.12% that of Hβ are also shown in Table 1 and labeled by "?".

Some permitted lines, e.g. O I λ6046, λ7002, λ7254, Si II λ5958, λ5979, λ6347, are likely of fluorescent origin and produced by absorption of the intense UV radiation (Esteban et al. 1998). Other lines (broad features at λ4620 and λ5700–5850) can be stellar in origin and likely produced by Wolf-Rayet stars. Weak He II λ4200 absorption

Table 1. Extinction-corrected fluxes of the emission lines in the brightest region.

λ_0(Å) Ion	λ_{obs}[a]	$I(\lambda)$[b]	λ_0(Å) Ion	λ_{obs}[a]	$I(\lambda)$[b]	λ_0(Å) Ion	λ_{obs}[a]	$I(\lambda)$[b]
3727 [O II]	3728	2136	4815 [Fe II]	4814	9	5876 He I	5875	1043
3750 H12	3751	393	4861 Hβ	4861	10 000	?	5917	4
3771 H11	3771	471	4907 [Fe IV]?	4904	22	?	5932	3
3798 H10	3798	597	4922 He I	4922	94	5958 Si II	5957	8
3820 He I	3820	75	4959 [O III]	4959	10 663	5979 Si II	5978	8
3835 H9	3836	798	5007 [O III]	5007	32 271	?	5999	3
3868 [Ne III]	3869	2349	5085 [Fe III]	5080	6	6046 O I	6044	5
3889 H8 + He I	3890	1741	?	5097	3	6074 He II	6075	3
3926 He I	3927	27	5112 [Fe II]	5112	6	?	6085	2
?	3943	31	5146 [Fe VI]	5149	15	6102 He II	6100	4
3968 [Ne III] + H7	3969	2478	5159 [Fe II], [Fe VII]	5160	15	?	6150	4
4009 He I	4009	11	5176 [Fe VI]	5181	7	6170 He II	6169	2
4026 He I	4027	137	5199 [N I]	5198	33	?	6270	3
4068–76 [S II]	4071	44	?	5214	3	6300 [O I]	6300	87
4101 Hδ	4102	2604	?	5235	5	6312 [S III]	6311	51
4121 He I	4122	16	?	5244	2	6347 Si II	6346	8
4144 He I	4145	20	5262 [Fe II]	5259	7	6363 [O I]	6363	32
4169 He I	4168	11	5271 [Fe III]	5270	242	6407 He II	6407	4
4227 [Fe V]	4228	36	?	5309	6	?	6455	9
4287 [Fe II]	4288	18	5335 [Fe VI]	5336	6	6563 Hα	6562	27 366
?	4314	12	?	5351	2	6678 He I	6677	260
4340 Hγ	4341	4753	?	5369	4	6717 [S II]	6716	197
4363 [O III]	4364	1089	?	5390	2	6731 [S II]	6731	166
4388 He I	4389	43	5411 He II	5412	13	7002 O I	7002	13
4415 [Fe II]	4416	12	5424 [Fe VI]	5424	2	?	7038	5
?	4434	10	?	5436	2	7065 He I	7065	427
4452 [Fe II]	4453	6	5485 [Fe VI]	5482	2	7136 [Ar III]	7135	212
4471 He I	4472	344	?	5501	5	7171 [Ar IV]	7170	7
4511 N III	4509	7	5517 [Cl III]	5517	13	?	7195	2
4565 Si III	4566	10	5538 [Cl III]	5537	10	?	7210	2
?	4581	8	?	5552	5	?	7224	2
4603-20 N V?, N III?	4609	32	?	5580	3	7237 [Ar IV]	7237	3
4640 N III	4641	13	?	5595	4	7254 O I	7254	10
4658 [Fe III]	4659	43	?	5608	3	7263 [Ar IV]	7264	5
4686 He II	4686	221	5639 [Fe VI]	5638	3	7281 He I	7280	52
4711 [Ar IV]+He I	4712	182	5677 [Fe VI]	5678	7	7298 He I	7295	5
4740 [Ar IV]	4741	104	?	5698	2	7320 [O II]	7319	60
4755 [Fe III]	4757	7	5721 [Fe VII]	5721	10	7330 [O II]	7330	28

[a] $\lambda_{obs} = \lambda_{measured}/(1+z)$, where $\lambda_{measured}$ is the measured wavelength of the emission line, $z = 0.0135$ is the redshift of SBS 0335–052.
[b] $I(\lambda)$ is normalized to the flux of $10^{-4} \times I(\mathrm{H}\beta)$.

is also detected, which is produced in the atmospheres of O stars. Although our detection level is comparable to that in deep spectra of Orion and planetary nebulae, optical recombination lines found in those objects (e.g. Esteban et al. 1998; Liu et al. 2000) are not detected here. This is likely due to the much lower metallicity of SBS 0335–052.

Several emission lines indicate the presence of intense hard radiation at energies above 54 eV ($\lambda < 228$ Å) and possibly even above 75–99 eV. The well-known He II λ4686 line and also He II λ5411 are detected. We confirm the presence of the forbidden [Fe V] λ4227 line, previously discovered in SBS 0335–052 and another low-metallicity BCD (Tol 1214–277) by Fricke et al. (2001). In addition several weak [Fe VI] and possibly [Fe VII] emission lines are detected in our spectrum. The ionization potentials corresponding to these Fe lines are 54.8, 75.0, and 99 eV respectively; the He^+ emitting region is therefore expected to be associated with the emission of [Fe V-VII]. The [Ar V] λ7006 line is likely detected. However, it is blended with O I λ7002 emission line. The possible identification of [Ar V] λ6435 line by Fricke et al. (2001) appears very uncertain from our spectrum.

The origin of hard radiation in giant H II regions has been debated for many years. Possible sources for this radiation include shocks, X-ray binaries, or hot Wolf-Rayet stars (cf. Garnett et al. 1991; Schaerer 1996). The spatial distribution of He II λ4686, [O III] λ4363, Hβ, and the adjacent continuum (see Fig. 2a) show some evidence for the presence of shocks, at least in a limited area of SBS 0335–052. Indeed, in the NW direction He II λ4686/Hβ remains relatively strong[2] out to the position of the ionized gas shell seen in HST images at a distance ∼6 arcsec from the two central clusters 1 and 5 of Thuan et al. (1997; cf. also Papaderos et al. 1998). Although expected, the other high excitation lines of [Fe V-VII] are too faint to be detected away from the main clusters. Furthermore, an increase of the electron temperature is observed away from the main clusters towards the shell (Fig. 2b), which may result from additional heating due to shocks. Both the extent of the region with He II λ4686/H$\beta \sim 0.06$ and the increase of T_e at large distance from the main ionizing clusters, where geometric dilution will greatly reduce the local ionization parameter, are suggestive of shocks in the area within and out to the shell. On the other hand, in the region centered on the main clusters we cannot distinguish between shocked and photoionized gas, as nearby

[2] The significance of the dip at position 3–4 arcsec and the reincrease in He II λ4686/Hβ to 6 arcsec is not large.

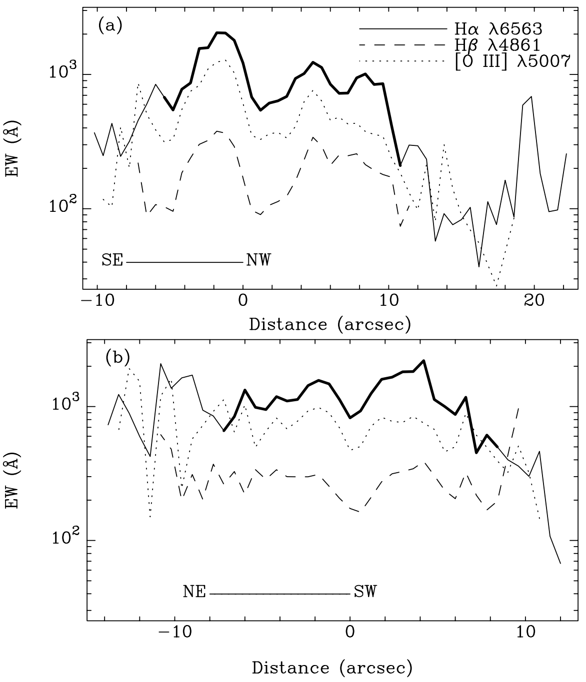

Fig. 3. a) Distribution along the slit of the equivalent widths of Hα (solid line), Hβ (dashed line) and [O III] λ5007 (dotted line) emission lines. The slit is oriented at position angle −30°. Thick solid line shows the range of the reliable EW(Hα). Outside this range the continuum is very weak, corresponging to R band surface brightness fainter 25 mag arcsec^{-2}. **b)** Same as **a)** but slit is oriented at position angle 80°.

stellar objects with hard ionizing spectra cannot be excluded. In passing we note that if shocks are present, the oxygen abundance gradient derived assuming a pure photoionized H II region model (Fig. 2b) may not be real. Observations of the spatial distribution of various high excitation lines (including [Fe V-VII] and [Ne V] λ3426 which is expected to be strong from shock models; e.g. Dopita & Sutherland 1996) as well as a detailed modeling are required to establish more firmly the importance of shocks on the spectrum of SBS 0335–052.

4. Extended nebular emission

Melnick et al. (1992) first obtained an Hα image of SBS 0335–052 and found that the ionized gas extends out to ∼7 arcsec, or over a region of ∼2 kpc in diameter. The deep long-slit Keck spectra of SBS 0335–052 allow us to trace ionized gas emission over a much larger region. In Fig. 3 we show spatial distributions of the equivalent widths in two nearly perpendicular directions of the brightest emission lines Hβ, Hα and [O III] λ5007. Hα emission is detected over 32 arcsec in the direction of PA = −30° and over 26 arcsec in the direction of PA = 80°. This corresponds to a linear size of 8 × 6 kpc, roughly the size of the 26 mag arcsec^{-2} R band isophote (Lipovetsky et al. 1999), or more than 3 times larger than that obtained from the Hα image by Melnick et al. (1992).

Very high equivalent widths of the emission lines in SBS 0335–052 (Fig. 3) imply that the contribution of the ionized gas to the total light is important and dominate in the regions with the largest equivalent widths. This finding shows, as already pointed out in several earlier studies (e.g. Krüger et al. 1995; Izotov et al. 1997; Papaderos et al. 1998), that both nebular continuum and line emission must be taken into account in photometric studies of stellar populations in the extended regions of BCDs. Obviously, the contribution of the emission lines to the total light depends on their relative strengths and redshift. H II region models predict a decrease of [O III] λ5007/Hβ with distance from the center due to a decreasing ionization parameter. This is observed in SBS 0335–052. If one assumes that the extended emission in SBS 0335–052 is only gaseous, then the $V-I$ colour is changed from ∼−0.6 mag in the center, where [O III] λ5007/Hβ ∼ 3.3, to ∼0.0 mag in outer regions, where [O III] λ5007/Hβ ∼ 1.5. In other words, even without stellar emission, the distribution of gaseous emission mimics a contribution of red stars increasing with distance. For analysis of stellar populations a proper removal of ionized gas emission is therefore crucial.

Acknowledgements. Y. I. I. has been partly supported by INTAS 97-0033 grant, and acknowledges support from the "Kiev project" of the Université Paul Sabatier of Toulouse. He is grateful for the hospitality of the Midi-Pyrénées Observatory where this work was conducted. The authors further wish to extend special thanks to those of Hawaiian ancestry on whose sacred mountain we are privileged to be guests. Without their generous hospitality, none of the observations presented herein would have been possible.

References

Dopita, M. A., & Sutherland, R. S. 1996, ApJS, 102, 161
Esteban, C., Peimbert, M., Torres-Peimbert, S., & Escalante, V. 1998, MNRAS, 295, 401
Fricke, K. J., Izotov, Y. I., Papaderos, P., Guseva, N. G., & Thuan, T. X. 2001, AJ, 121, 169
Garnett, D. R., Kennicutt, R. C. Jr., Chu, Y.-H., & Skillman, E. D. 1991, ApJ, 373, 458
Izotov, Y. I., Chaffee, F. H., Foltz, C. B., et al. 1999, ApJ, 527, 757
Izotov, Y. I., Lipovetsky, V. A., Chaffee, F. H., et al. 1997, ApJ, 476, 698
Izotov, Y. I., Lipovetsky, V. A., Guseva, N. G., Kniazev, A. Y., & Stepanian, J. A. 1990, Nature, 343, 238
Krüger, H., Fritze-v. Alvensleben, U., & Loose, H.-H. 1995, A&A, 303, 41
Lipovetsky, V. A., Chaffee, F. H., Izotov, Y. I., et al. 1999, ApJ, 519, 177
Liu, X.-W., Storey, P. J., Barlow, M. J., et al. 2000, MNRAS, 312, 585
Melnick, J., Heydari-Malayeri, M., & Leisy, P. 1992, A&A, 253, 16
Oke, J. B., Cohen, J. G., Carr, M., et al. 1995, PASP, 107, 375
Papaderos, P., Izotov, Y. I., Fricke, K. J., Guseva, N. G., & Thuan, T. X. 1998, A&A, 338, 43
Schaerer, D. 1996, ApJ, 467, L17
Thuan, T. X., Izotov, Y. I., & Lipovetsky, V. A. 1997, ApJ, 477, 661